Article

Cell Reports

Expression Quantitative Trait Loci and Receptor Pharmacology Implicate Arg1 and the GABA-A Receptor as Therapeutic Targets in Neuroblastoma

Graphical Abstract

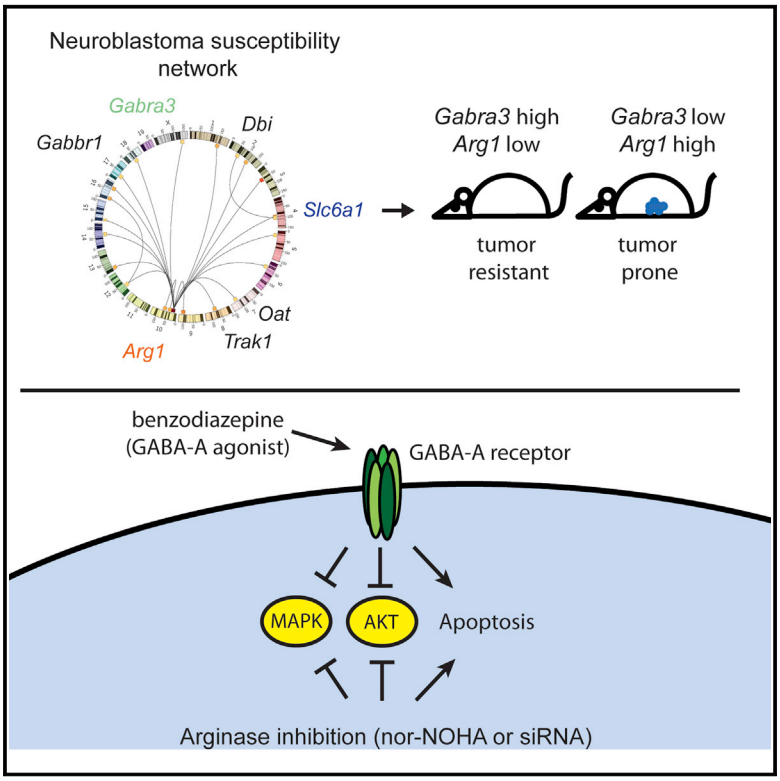

Highlights

Arg1 and GABA gene expression correlates with neuroblastoma formation in mice

GABA gene expression correlates with survival in human neuroblastomas

Both activation of GABA-A and inhibition of ARG1 block the growth of neuroblastoma cells

A benzodiazepine inhibits AKT and ERK and induces apoptosis in neuroblastoma cells

Authors

Christopher S. Hackett, David A. Quigley, ..., QiWen Fan, William A. Weiss

Correspondence

qiwen.fan@ucsf.edu (Q.F.), waweiss@gmail.com (W.A.W.)

In Brief

Neuroblastoma is a pediatric tumor of peripheral neural tissue. Hackett et al. now link *Arg1* and GABA with genetic susceptibility to neuroblastoma formation in mice. Expression of GABA genes correlates with survival in human tumors. GABA activation and ARG1 inhibition block the growth of neuroblastoma cells. These results identify therapeutic targets in neuroblastoma and suggest a role for these pathways in neural growth.

Accession Numbers

GSE59675

Hackett et al., 2014, Cell Reports 9, 1034–1046
November 6, 2014 ©2014 The Authors
http://dx.doi.org/10.1016/j.celrep.2014.09.046

OPEN ACCESS
CellPress

Cell Reports
Article

Expression Quantitative Trait Loci and Receptor Pharmacology Implicate Arg1 and the GABA-A Receptor as Therapeutic Targets in Neuroblastoma

Christopher S. Hackett,[1,2] David A. Quigley,[3] Robyn A. Wong,[2] Justin Chen,[1,2] Christine Cheng,[2] Young K. Song,[4] Jun S. Wei,[4] Ludmila Pawlikowska,[5,6] Yun Bao,[2] David D. Goldenberg,[2] Kim Nguyen,[2] W. Clay Gustafson,[7] Sundari K. Rallapalli,[8] Yoon-Jae Cho,[9] James M. Cook,[8] Serguei Kozlov,[10] Jian-Hua Mao,[11] Terry Van Dyke,[10] Pui-Yan Kwok,[6,12,13] Javed Khan,[4] Allan Balmain,[3] QiWen Fan,[2,*] and William A. Weiss[2,7,14,*]

[1]Biomedical Sciences Graduate Program, University of California, San Francisco, San Francisco, CA 94143, USA
[2]Department of Neurology, University of California, San Francisco, San Francisco, CA 94143, USA
[3]Helen Diller Family Comprehensive Cancer Center, University of California, San Francisco, San Francisco, CA 94143, USA
[4]Oncogenomics Section, Pediatric Oncology Branch, National Cancer Institute, Gaithersburg, MD 20877, USA
[5]Department of Anesthesia, University of California, San Francisco, San Francisco, CA 94143, USA
[6]Institute for Human Genetics, University of California, San Francisco, San Francisco, CA 94143, USA
[7]Department of Pediatrics, University of California, San Francisco, San Francisco, CA 94143, USA
[8]Departments of Chemistry and Biochemistry, University of Wisconsin-Milwaukee, Milwaukee, WI 53211, USA
[9]Department of Neurology, Stanford University School of Medicine, Stanford, CA 94305, USA
[10]Mouse Cancer Genetics Program, Center for Advanced Preclinical Research, National Cancer Institute, Frederick, MD 21702, USA
[11]Department of Epidemiology and Biostatistics, University of California, San Francisco, San Francisco, CA 94143, USA
[12]Department of Dermatology, University of California, San Francisco, San Francisco, CA 94143, USA
[13]Cardiovascular Research Institute, University of California, San Francisco, San Francisco, CA 94143, USA
[14]Department of Neurological Surgery, University of California, San Francisco, San Francisco, CA 94143, USA
*Correspondence: qiwen.fan@ucsf.edu (Q.F.), waweiss@gmail.com (W.A.W.)
http://dx.doi.org/10.1016/j.celrep.2014.09.046

SUMMARY

The development of targeted therapeutics for neuroblastoma, the third most common tumor in children, has been limited by a poor understanding of growth signaling mechanisms unique to the peripheral nerve precursors from which tumors arise. In this study, we combined genetics with gene-expression analysis in the peripheral sympathetic nervous system to implicate arginase 1 and GABA signaling in tumor formation in vivo. In human neuroblastoma cells, either blockade of ARG1 or benzodiazepine-mediated activation of GABA-A receptors induced apoptosis and inhibited mitogenic signaling through AKT and MAPK. These results suggest that ARG1 and GABA influence both neural development and neuroblastoma and that benzodiazepines in clinical use may have potential applications for neuroblastoma therapy.

INTRODUCTION

Neuroblastoma, a common and deadly pediatric tumor of the peripheral nervous system, is derived from sympathetic neural progenitors that normally differentiate into postmitotic neurons. This tumor likely arises from disruption of growth pathways specific to the neural lineage, as mutations in canonical growth pathways seen in epithelial, glial, and hematopoietic tumors are rarely observed. Amplification of the *MYCN* proto-oncogene is a hallmark of high-risk neuroblastoma (Brodeur et al., 1984; Schwab et al., 1984), and a transgenic mouse model driven by MYCN develops tumors with histological and genomic characteristics of human neuroblastoma (Hackett et al., 2003; Weiss et al., 1997). In this model, tumor incidence varies among mouse strains, with the strain FVB/N showing complete resistance to tumor formation.

In this study, we exploited this genetic variance to identify molecular pathways that drive neuroblastoma development. We first identified tumor susceptibility loci through classical genetic linkage mapping in genetically heterogeneous backcross mice. We next analyzed gene expression as a function of genetic variation to identify expression quantitative trait loci (eQTLs) in sympathetic superior cervical ganglia (SCGs) in these mice. We then used eQTLs localizing to tumor susceptibility loci to identify candidate tumor susceptibility genes. Liver arginase (*Arg1*), a component of both the urea cycle and the gamma-amino butyric acid (GABA) biosynthetic pathway, was the strongest eQTL at the most prominent tumor susceptibility locus. Multiple genes and eQTLs involved in GABA neurotransmitter signaling were located at secondary susceptibility loci, providing an intriguing genetic link between this pathway and neuroblastoma biology. We validated this link using compounds targeting the ARG1-GABA pathway in human neuroblastoma cell lines. Nor-NOHA, an ARG1 inhibitor, inhibited the growth and viability of cells. More strikingly, activation of GABA-A signaling using a benzodiazepine derivative induced apoptosis and was

associated with decreased activity of PI3K/AKT and MAPK signaling pathways, both of which play a central role in cell growth and survival. These data implicating arginine metabolism and GABA signaling in the pathogenesis of neuroblastoma present a combination of novel therapeutic targets. Additionally, the demonstration that the neurotransmitter GABA inhibits the growth of tumor cells derived from a neural lineage highlights an emerging role for neurotransmitters in regulating development of the peripheral nervous system.

RESULTS

The Penetrance of Neuroblastoma in TH-MYCN Mice Is Strain Dependent

Transgenic mice were generated on a Balb/c × C57B6/J background with ~10% incidence of tumors. After two backcrosses into strain FVB/NJ, tumor incidence decreased to zero (Figure S1A). Conversely, tumor incidence increased steadily with each successive backcross into strain 129/SvJ, to ~60% (Chesler et al., 2007). The levels of transgene expression were similar between strains (Figure S1B).

We crossed resistant transgenic FVB/NJ mice to susceptible wild-type 129/SvJ. Four percent of F1 mice developed tumors, suggesting that resistance was dominant. To generate a genetically diverse population for linkage mapping, we backcrossed transgenic F1 animals to wild-type 129/SvJ mice. The incidence of tumors in the resulting N1 backcross generation was 38% (n = 203), with an average survival (109 days) identical to that of mice carrying the transgene in a pure 129/SvJ background (Figure S1C; Chesler et al., 2007).

Linkage Analysis Identifies a Tumor Susceptibility Modifier on Chromosome 10

To identify genomic loci associated with tumor susceptibility, we genotyped 203 mice using a combination of microsatellite and SNP markers (Table S1). Interval mapping for linkage to tumor susceptibility produced a maximum LOD (log of odds) score on chromosome 10 at marker RS36323433 (LOD = 4.1, significant at a 5% genome-wide error rate). Interestingly, tumor susceptibility was strongly influenced by gender. Sex as an interacting covariate increased the LOD score to 4.9 (Figures 1A and 1B). This locus was significant in male mice (LOD = 4.3, n = 82), but not in female mice. It may be relevant in this regard that neuroblastoma is slightly more prevalent in boys (1.3:1) than in girls (Hale et al., 1994). Contrary to the expected allele segregation at this locus, heterozygous mice were tumor prone (55%), whereas mice homozygous for the 129/SvJ alleles were resistant (25% incidence; Figures 1C and S1D). The absence of a single locus at which an FVB/N allele conferred complete resistance to tumor formation (a trait of FVB/N mice) suggested that the genetics underlying patterns of resistance and susceptibility in pure inbred strains is complex.

Since the segregation of genotypes with tumor susceptibility at the chromosome 10 locus did not match the patterns of tumor susceptibility in the parent strains, we next considered a more complex genetic model to explain susceptibility. A two-QTL test identified several loci that interacted with the chromosome 10 locus, with similar LOD scores (Figures 1D and 1E; Table S2). Interestingly, although all of these loci interacted with the chromosome 10 locus, they did not interact with each other.

eQTL Analysis Identifies *Arg1* as a Candidate Modifier

The 95% confidence interval (CI) of the peak on chromosome 10 spanned 47 Mb and contained more than 281 genes, complicating identification of candidates. Hypothesizing that susceptibility to tumors may be governed by differential expression of genes within this locus, we compared mRNA expression levels in neural-crest-derived sympathetic SCGs from transgenic 129/SvJ and FVB/NJ male mice. We identified 9,819 genes that were differentially expressed genome-wide between the two strains (Figure S1C; Table S3), including 137 within the 95% CI for the chromosome 10 susceptibility locus (representing almost half of all genes within the locus). Surprisingly, when male and female 129/SvJ and FVB/NJ mice were compared, only six genes were differentially expressed between sexes. With the exception of a RIKEN clone on chromosome 2, all mapped to either the X or Y chromosomes (Figure S1D; Table S3), excluding gender-specific gene expression as a mechanism for the gender effect at the chromosome 10 locus.

Gene-expression levels can be influenced by complex interactions among *cis*- and *trans*-acting factors. Such factors can be distinguished by identifying eQTLs, which involves generating a genetically heterogeneous population (such as our backcross population), measuring gene-expression levels, and treating the expression level of each gene as a quantitative trait for subsequent linkage mapping (Brem et al., 2002; Schadt et al., 2003). Through this method, *cis*- and *trans*-acting alleles that influence gene expression are decoupled from each other, and genes whose differential expression is due to *cis*-acting factors at a locus can be distinguished from genes under the control of *trans*-acting factors at other loci. Genes with eQTLs overlapping with QTLs for physiological phenotypes have been shown to control these phenotypes (Schadt et al., 2003; Yang et al., 2009). Therefore, we utilized this technique to identify eQTLs within our chromosome 10 locus, as well as at the numerous other secondary loci identified in the two-QTL tumor susceptibility analysis.

We measured mRNA expression levels in 116 SCGs from the backcross population and tested for linkage between gene-expression levels and germline genetic variation. We identified 342 eQTLs acting both locally and on other chromosomes (Table S4). Four eQTLs mapped to the susceptibility locus on chromosome 10, with *Arg1* (liver arginase) showing the strongest eQTL. When this measurement was refined by interval mapping, *Arg1* expression was linked to a QTL at chromosome 10 with a LOD score of 18.2 (Figure 2A). Mice heterozygous at that locus had almost 2-fold higher expression of *Arg1* compared with mice homozygous for the 129/SvJ allele (Figures 2B and S2A). Of the four eQTLs that mapped to the locus, the *Arg1* eQTL overlapped most directly and with the highest LOD score (Figures S2B and S2C), making *Arg1* our top candidate gene (Figure 2C; Table 1). Notably, among 137 genes differentially expressed at the chromosome 10 locus in parental strains, only four, including *Arg1*, showed significant eQTL mapping to the locus (Table S4). These data suggest that the differential expression of the other

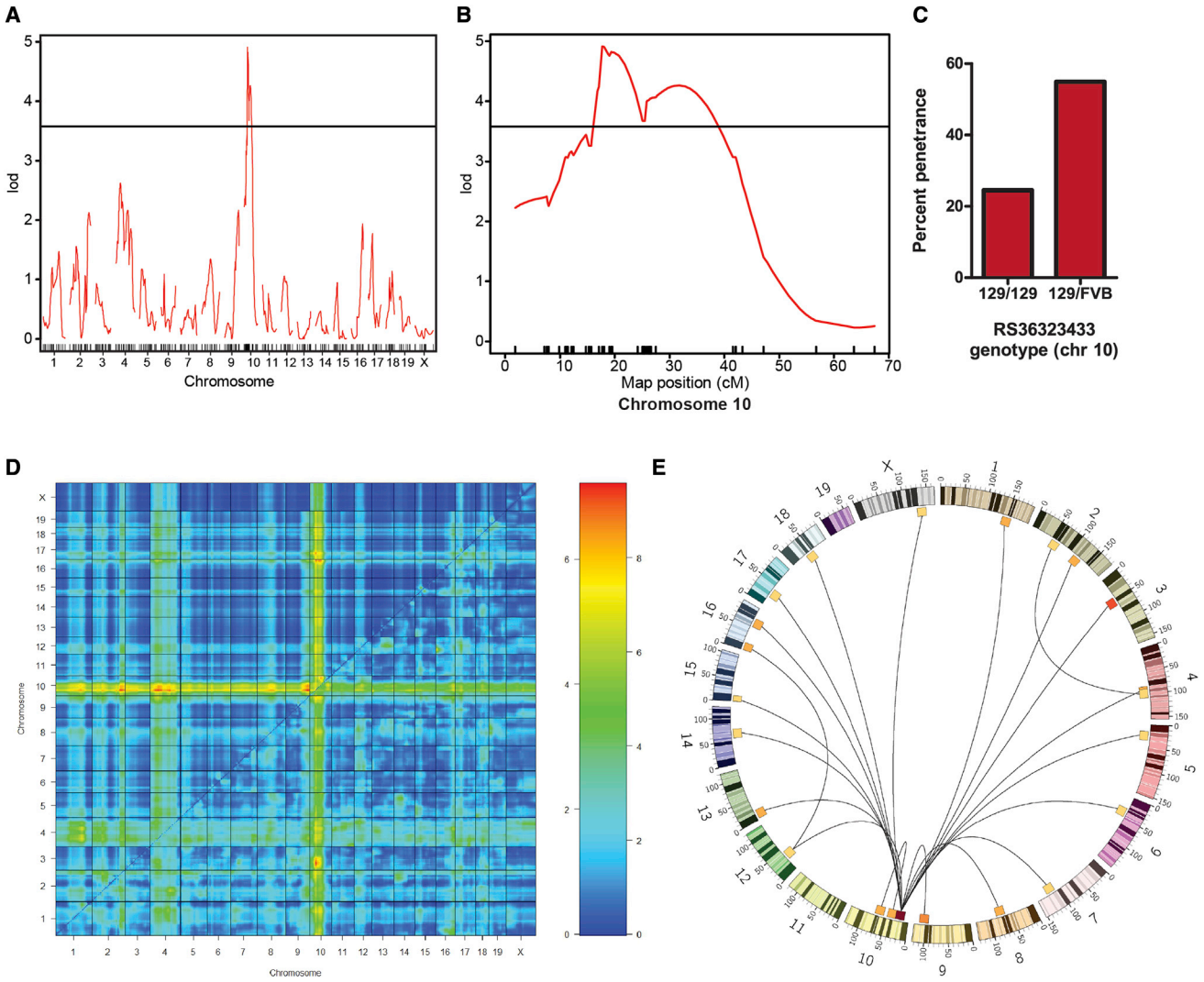

Figure 1. A Locus on Chromosome 10 and Multiple Secondary Loci Are Linked to Tumor Susceptibility

(A) A LOD plot for tumor susceptibility shows a single significant locus on chromosome 10. Horizontal line indicates 5% genome-wide significance threshold (LOD = 3.58, 1,000 permutations).

(B) LOD plot of chromosome 10 only. Hash marks on the horizontal axis indicate marker positions. Horizontal line indicates 5% genome-wide significance threshold (LOD = 3.58, 1,000 permutations).

(C) Effect plot for the marker closest to the maximum LOD score (RS36323433) showing incidence of tumors as a function of genotype.

(D) Two-QTL analysis using sex as an interacting covariate reveals that multiple secondary loci interact with the chromosome 10 locus. The top-left half shows the results of the additive model, and the bottom-right half shows results of the "full" model. The bar on the right displays the correspondence between color on the chart and LOD scores (the left side of the bar corresponds to the additive analysis on the top-left half of the plot, while the right side of the bar, with a different scale, corresponds to the full model analysis on the bottom right). Locations of the maximum LOD scores are shown in Table S2.

(E) Circos plot illustrating the two-way interactions shown in (D). Pairs of loci with an LOD > 6 are connected.

See also Figure S1 and Table S1.

genes in the parents was due in part to *trans*-acting factors, illustrating the power of eQTL analysis for dissecting control of gene expression at a genetic locus and filtering candidate genes.

eQTLs for GABA-Related Genes Map to Secondary Susceptibility Loci

We next looked for eQTLs that mapped to secondary tumor susceptibility loci that interacted with the chromosome 10 locus. We noted eQTLs for genes related to GABA neurotransmitter signaling at two of the loci (Table 1). Notably, a *trans* eQTL on chromosome 2 controlled expression of the *Gabra3* receptor subunit on the X chromosome (Figures 3A–3C). This eQTL overlapped directly with the secondary susceptibility locus on chromosome 2 (Figure S3A; Table 1). Mice harboring alleles resulting in high *Arg1* expression and low *Gabra3* expression showed the strongest susceptibility to tumors (Figure 3C). Similarly, an eQTL

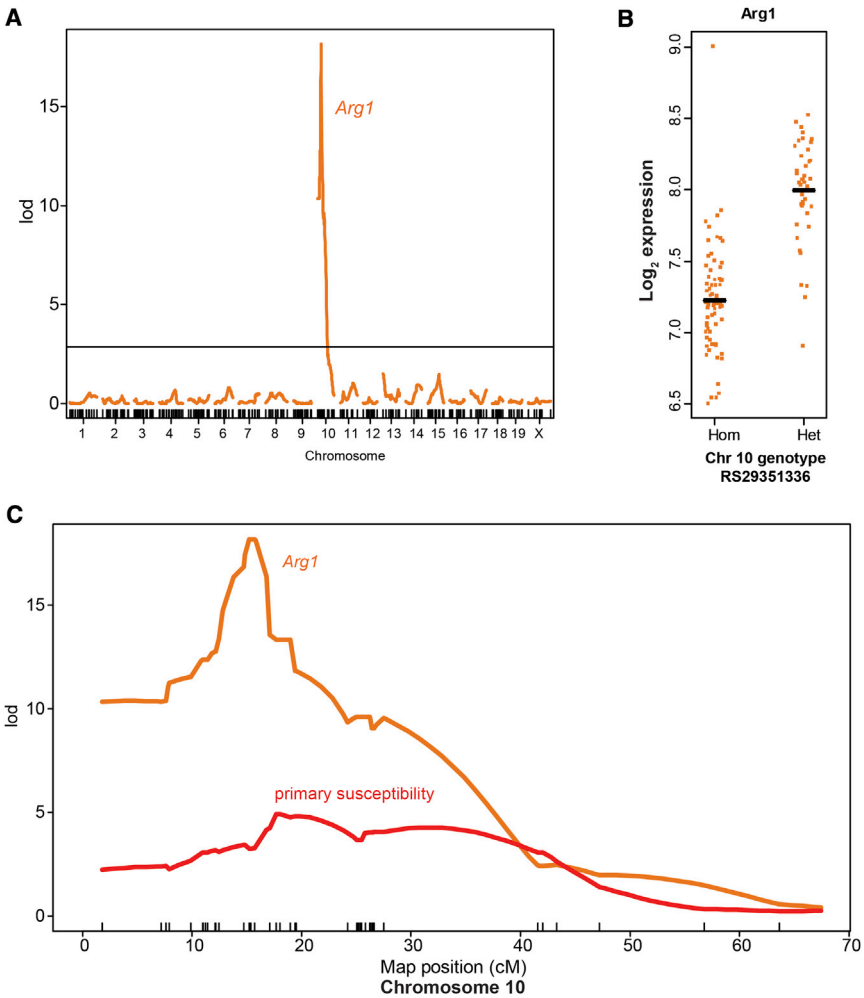

Figure 2. An eQTL for *Arg1* Colocalizes with the Tumor Susceptibility Locus on Chromosome 10

(A) Interval mapping for expression of *Arg1*, the most significant eQTL in the chromosome 10 region, showing a LOD score of 18.2 on chromosome 10 centered at the physical location of the *Arg1* gene. Horizontal line indicates 5% genome-wide significance threshold.

(B) Log_2 *Arg1* expression level as a function of genotype at SNP RS29351336 on chromosome 10.

(C) A plot of LOD scores on chromosome 10 for susceptibility (red line) and the *Arg1* eQTL (orange line) showing colocalization of the peaks.

See also Tables S3 and S4.

for the GABA transporter *Slc6a1* (Figures 3D–3F) mapped to a secondary susceptibility locus on chromosome 4 (Figure S3B; Table 1), though the gene was on chromosome 6. We noted that the differences in gene expression of *Gabra3* and *Slc6a1* were also apparent in the parental strains (Figures S3C and S3D). The overlap of *Gabra3*, *Slc6a1*, and *Arg1* eQTLs with primary and secondary susceptibility loci is illustrated genome-wide in Figure 3G.

We next investigated secondary susceptibility loci that lacked GABA-related eQTL candidates, and found several GABA-related genes that mapped within 10 Mb of susceptibility peaks. The locus on chromosome 1 (LOD 7.8) flanked by markers RS5056599 (116 Mb) and D1MIT1001 (131 Mb, LOD 7.8) lies in close proximity to *Dbi* (diazepam binding inhibitor, 122 Mb), a gene that modulates GABA receptor activity (Gray et al., 1986). Similarly, the locus on chromosome 9 centered near 117 Mb (D9MIT201, LOD 7.9) is 4 Mb from the *Trak1* gene, which encodes a trafficking factor that modulates GABA receptor homeostasis (Gilbert et al., 2006). The locus on chromosome 7 centered at 144 Mb (RS13479509, LOD 6.4) is 4 Mb from ornithine aminotransferase (*Oat*), which converts ornithine to glutamate (the substrate for GABA synthesis). Finally, the locus on chromosome 17 centered near 35 Mb (D17MIT231, LOD 6.7) is 2 Mb from the GABA-B receptor 1. Altogether, at least six secondary susceptibility loci colocalized with genes in the GABA pathway or eQTLs that controlled these genes (Table 1).

Expression of GABA Pathway Genes Identified by Linkage and eQTL Analysis Predicts Survival in Neuroblastoma

We next investigated whether expression of *ARG1* and the GABA pathway genes correlated with outcomes in human neuroblastoma. We analyzed a database of gene-expression profiles of human neuroblastoma samples (Asgharzadeh et al., 2006; available at http://home.ccr.cancer.gov/oncology/oncogenomics). Strikingly, all of the genes in the GABA pathway that either mapped to tumor susceptibility loci or were controlled by eQTLs at these loci showed a significant correlation with survival (Figures 4A–4F). *ARG1* did not show a strong correlation with survival in human neuroblastomas (Figure 4G). However, the population was relatively homogeneous with respect to *ARG1* expression (Figure 4H), hindering our ability to segregate tumors based on expression levels.

Inhibition of ARG1 Decreases the Viability of Human Neuroblastoma Cells

The higher-expressing Arginase allele that confers tumor susceptibility is nested within an overall resistant genetic background in purebred mice (either FVB/NJ or FVB/NJ × 129/SvJ F1). The allelic variation in secondary loci (harboring components of the GABA pathway) only showed an effect in combination with alleles at other loci. This genetic complexity precluded validation in vivo. Therefore, we used an in vitro approach to test whether these biochemical pathways have relevance to human tumor biology. Since little is known about the role of these pathways in regulating cell growth and thus there is little basis for

Table 1. Candidate Genes at Susceptibility Loci

Candidate eQTLs at Susceptibility Loci

Chr	Susceptibility Locus (Mb)	LOD	eQTL Gene	eQTL Locus (Mb)	eQTL p Value	Permutation p Value
10	28	5.0	Arg1	25	2.92×10^{-20}	<0.001
2	166	7.0	Gabra3	178	5.57×10^{-34}	<0.001
4	115	7.4	Slc6a1	129	2.81×10^{-05}	0.001

Non-eQTL GABA Genes at Susceptibility Loci

Chr	Susceptibility Locus (Mb)	LOD	Gene	Gene Location (Mb)
1	131	7.8	*Dbi*	122
9	117	7.8	*Trak1*	121
17	35	6.9	*Gabbr1*	37
7	144	6.3	*Oat*	140

Gene Descriptions

Gene	Location (chr)	Description
Arg1	10	liver arginase
Gabra3	X[a]	GABA-A receptor, subunit alpha 3
Slc6a1	6[a]	GABA transporter, removes GABA from synaptic cleft
Dbi	1	diazepam binding inhibitor; modulates the action of the GABA receptor
Trak1	9	trafficking protein, kinesin binding 1, regulates GABA receptor
Gabbr1	17	GABA-B receptor, 1
Oat	7	ornithine aminotransferase (produces glutamate, a GABA precursor)

Chr, chromosome.
[a]Controlled by *trans* eQTL.

identifying the specific downstream pathways involved, we assessed the effect of compounds targeting this pathway on overall growth and viability.

We detected ARG1 by western blot across a panel of human neuroblastoma cell lines (Figure 5A). We treated two lines, Kelly and CHP-126, with the reversible arginase inhibitor nor-NOHA (N-Omega-hydroxy-nor-arginine) (Tenu et al., 1999) to test whether inhibition of arginase could impair tumor growth. Viability was decreased in CHP-126 and Kelly cells across a range of doses from 1 μM to 100 μM (Figure 5B). Since nor-NOHA is not a particularly potent inhibitor in neuroblastoma cell lines, we next tested small interfering RNA (siRNA) against *ARG1*. *ARG1* siRNA induced a significant decrease in growth, an increase in the apoptotic markers Annexin V and cleaved PARP, and reduced levels of phosphorylated AKT and ERK, both of which are central components of mitogenic signaling pathways (Figures 5C and S4B). We next tested whether overexpression of ARG1 had the opposite effect. While overexpression alone did not produce a notable effect on growth, it did increase levels of phosphorylated AKT and ERK, and partially rescued the inhibitory effect of the benzodiazepine QHii066 (described below) (Figures 5D and S4C). We conclude that ARG1 expression modulates viability and proliferation in human neuroblastoma cells.

GABA-A Activation Induces Apoptosis in Neuroblastoma

We next investigated the role of GABA signaling in the control of cell growth and survival. GABA-A and GABA-B receptors were detected in all cell lines tested (Figures 5A and S4A). To assess whether modulation of this pathway influenced cell growth and survival, we treated cells with a potent and selective GABA-A receptor agonist, QHii066, a benzodiazepine derivative (He et al., 2000; Huang et al., 2000). QHii066 slowed cell growth and induced apoptosis in a dose-dependent fashion in both LAN-5 (Figure 5E) and Kelly (Figure S4D). Immunoblotting revealed increased PARP cleavage and reduced the abundance of phosphorylated AKT and ERK in cells treated with QHii066. Flow cytometry demonstrated G_0/G_1 arrest (Figure S4E). These data suggest that specific activation of the GABA-A receptor decreases cell viability, induces apoptosis, and suppresses growth and survival signaling pathways in neuroblastoma cell lines.

DISCUSSION

The pathways that regulate development of the peripheral nervous system are distinct from those that control other cell types. As a consequence, common genomic aberrations that drive tumorigenesis in epithelial, hematopoietic, and glial tumors rarely show abnormalities in neuroblastoma, a tumor of the sympathetic peripheral nervous system. Genetic analysis in humans and model systems has been key for identifying mechanisms that drive the disease. Here, we used a genetically engineered mouse model for neuroblastoma to uncover a signaling pathway relevant to human disease.

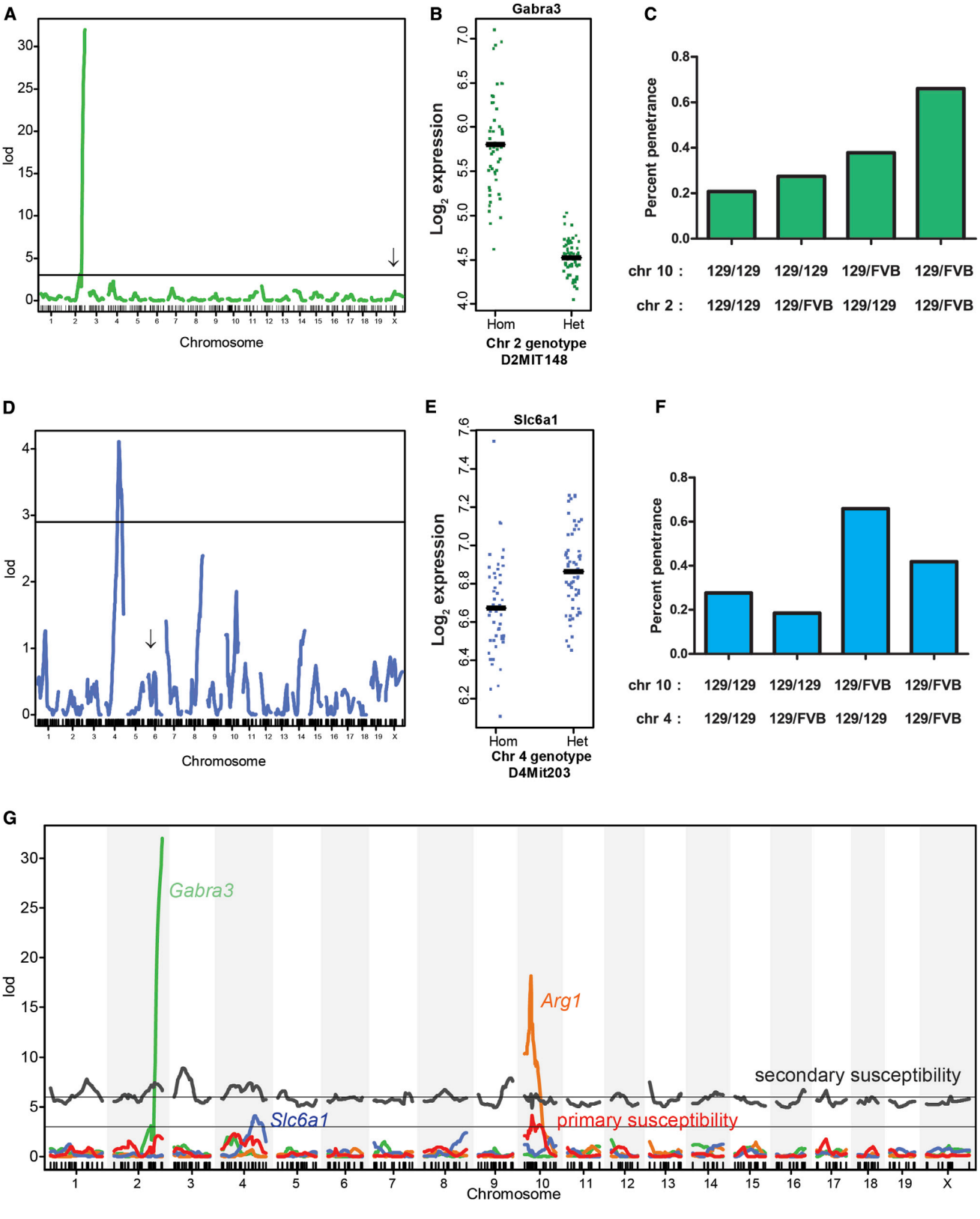

(legend on next page)

Although the influence of strain background on tumor penetrance is frequently observed in mouse models of cancer, few genes underlying this susceptibility have been identified (Crawford et al., 2008a; Ewart-Toland et al., 2003; MacPhee et al., 1995; Mao et al., 2006; Park et al., 2005; Wakabayashi et al., 2007), mostly due to the limited resolution of quantitative trait linkage mapping. Analysis of gene expression as a function of genotype (i.e., treating gene-expression levels as heritable traits and performing linkage analysis) has facilitated the identification of genes underlying physiological variation (Brem et al., 2002; Schadt et al., 2003; Yang et al., 2009). eQTL analysis has identified several genes that modify tumor susceptibility in mouse models of cancer (Crawford et al., 2008b; La Merrill et al., 2010; Quigley et al., 2009). In the current study, eQTL analysis of the peripheral nervous system identified *Arg1* as a candidate neuroblastoma modifier gene at chromosome 10, as well as a particularly prominent eQTL on chromosome 2 that governs the expression of a GABA-A neurotransmitter receptor subunit in *trans* on the X chromosome (a phenomenon that would have been missed by conventional analysis of candidate genes at the susceptibility loci). Numerous other susceptibility loci overlapped with other GABA-related genes, suggesting a mechanism for the pattern of genetic linkage to tumor susceptibility, and implicating an interaction between upregulation of arginase activity and downregulation of GABA receptors as cooperating mechanisms that promote susceptibility to tumors.

Although *Arg1* is associated with the urea cycle in liver, expression of *Arg1* in sympathetic nerve ganglia (Yu et al., 2003) that do not carry out the urea cycle suggested a role in other biochemical pathways. In neurons, *Arg1* is part of the GABA synthesis pathway, which produces ornithine, a precursor of glutamate and GABA. The biochemical link between *Arg1* and the GABA pathway potentially explains the unique genetic pattern of several secondary loci interacting with a single gene/locus. Only one cytoplasmic arginase gene exists (*Arg1*). However, the GABA signaling pathway may be perturbed at numerous genomic loci, including several components of the GABA-A receptor, genes for which are dispersed throughout the genome. Thus, in a genetic model involving perturbation of arginase and GABA signaling, many GABA-related genes could interact with the single *Arg1* gene on chromosome 10 with similar effects (disrupting two connected pathways), while GABA genes may not interact with each other (as multiple disruptions would have redundant effects on the same pathway). This model is consistent with the pattern of genetic interactions we observed in our system.

Several downstream outputs of the arginase pathway could account for increased expression of *Arg1* predisposing mice to tumors. Arginase may act as an immunosuppressant (Bak et al., 2008; Yachimovich-Cohen et al., 2010) or alter levels of nitric oxide synthases (Ciani et al., 2004; Jenkins et al., 1995). It may also alter levels of ornithine, the substrate for polyamine synthesis, which has been linked to tumorigenesis (Gerner and Meyskens, 2004) and neural proliferation (Huang et al., 2007). The rate-limiting polyamine synthetic enzyme ornithine decarboxylase (ODC) is a well-established target for MYCN (Bello-Fernandez et al., 1993). ODC inhibitors inhibit neuroblastoma development in vitro and in TH-*MYCN* mice (Hogarty et al., 2008; Koomoa et al., 2008), and are currently in clinical trials for neuroblastoma (http://clinicaltrials.gov/show/NCT01586260). Ornithine is also a substrate for synthesis of glutamate and GABA. Notably, ornithine aminotransferase (*Oat*), which converts ornithine to glutamate, maps to a susceptibility locus on chromosome 7 (Table 1). Since GABA inhibits neuronal growth and promotes differentiation (Andäng et al., 2008), at least one ultimate output of Arg1 activity (GABA) could inhibit both the induction and further growth of tumors, driving selection for secondary genetic lesions that disable this pathway.

Although Arg1 activity has not been studied extensively in cancer, inhibition of arginase has been shown to disrupt the growth of breast cancer cells (Singh et al., 2000). Arginase expression has also been linked to neuronal viability. Clinically, *ARG1* mutations cause arginemia, which is characterized by neurodegeneration (OMIM 207800). Although it has been speculated that this neurodegeneration is caused by hepatic production of neurotoxic metabolites (De Deyn et al., 1991; Deignan et al., 2008), our data, coupled with the detection of *Arg1* expression in neural tissues (Yu et al., 2001, 2002, 2003), suggest that *Arg1* may be involved in growth and survival signaling in neuroblasts, and inhibition of Arg1 may have an intrinsic cytotoxic effect in neurons and neuroblastoma cells.

The observation that mice with lower expression of GABA-A receptor subunits are tumor prone is consistent with GABA's known role in neuronal cell growth and differentiation (Andäng et al., 2008; Le-Corronc et al., 2011), and suggests that the association of downregulation of GABA-A receptors with aggressive human neuroblastomas has biological significance (Roberts et al., 2004). However, since the receptor is formed as a pentameric combination of 19 possible subunits with changing expression patterns and biological roles (Le-Corronc et al., 2011), testing this hypothesis is not straightforward. GABA signaling negatively regulates the growth of neural crest

Figure 3. Secondary Susceptibility Loci Colocalize with eQTL for GABA-Related Genes

(A) A *trans* eQTL on chromosome 2 controls expression of the GABA-A receptor subunit 3 (*Gabra3*) on the X chromosome (arrow) (LOD = 30.9).

(B) *Gabra3* expression as a function of D2MIT148 genotype.

(C) Plot of tumor incidence as a function of genotypes at the chromosome 2 and 10 loci.

(D) Expression QTL for the *Slc6a1* GABA transporter on chromosome 4 (LOD = 4.1). The arrow indicates the physical location of *Slc6a1* on chromosome 6.

(E) *Slc6a1* expression as a function of D4MIT203 genotype.

(F) Tumor incidence as a function of genotypes at loci on chromosomes 4 and 10.

(G) Genome-wide plot of LOD scores for the *Gabra3* (green), *Slc6a1* (blue), and *Arg1* (orange) eQTLs, and tumor susceptibility for a single-locus model (red) and the combined effect of the peak of the chromosome 10 locus plus points across the rest of the genome (gray), showing correspondence between eQTL peaks and primary and secondary susceptibility loci. 2D plots for *Gabra3* and *Slc6a1* are shown in Figure S3.

See also Figure S2 and Table S4.

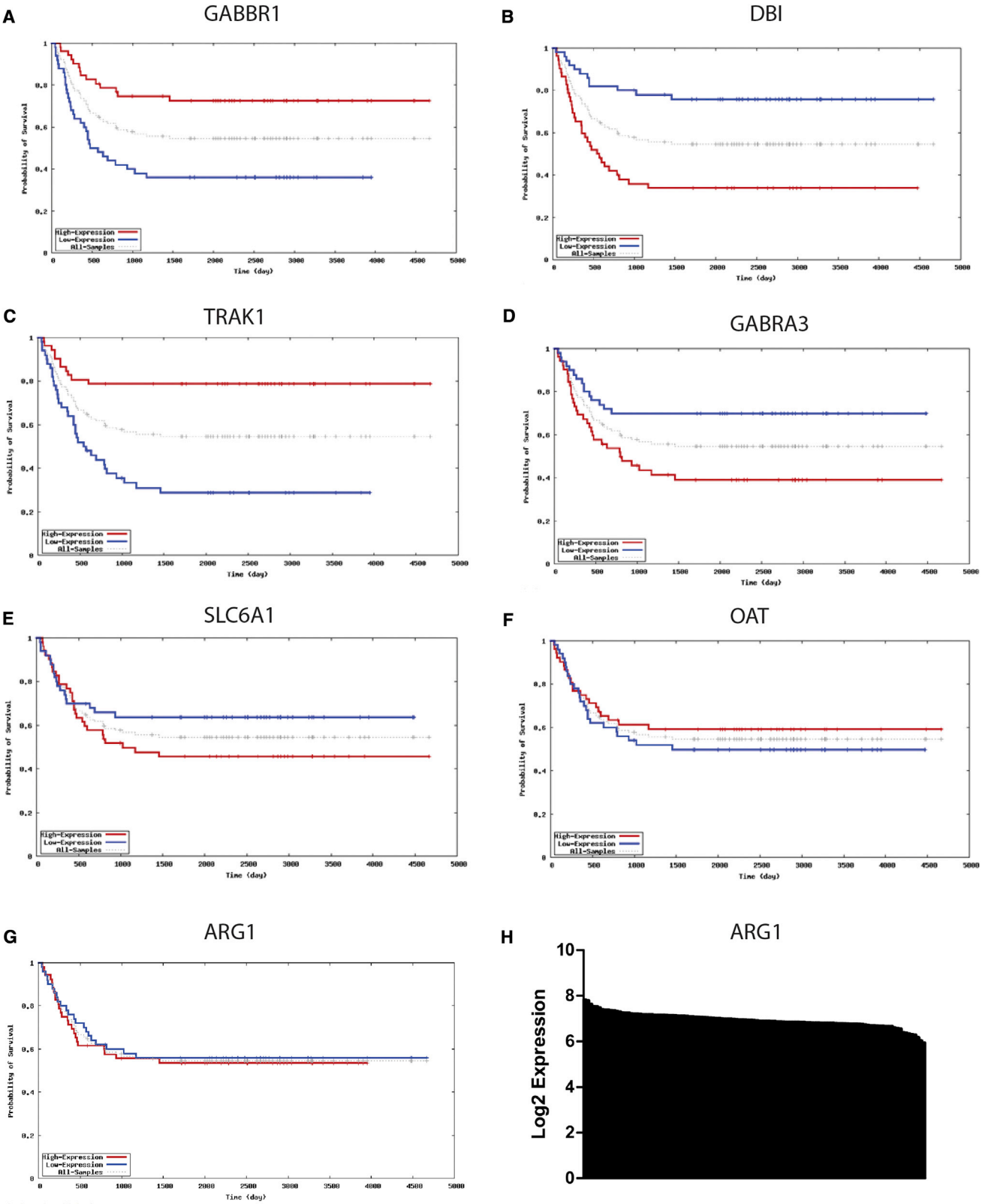

(legend on next page)

stem cells (Andäng et al., 2008). In our hands, neuroblastoma cells expressing the GABA-A receptor showed decreased viability, increased apoptosis, and diminished activity of mitogenic signaling pathways in response to GABA-A activation, supporting a role of GABA signaling in tumor cell growth and survival.

Neuroblastoma is a common pediatric tumor with a unique biology, making the development of novel targeted therapeutics problematic. As a result, improvements in clinical outcomes have been modest over the last several decades. Familial studies have identified genes that drive neuroblastoma, such as *ALK* (Janoueix-Lerosey et al., 2008; Mossé et al., 2008) and *PHOX2B* (Mosse et al., 2004; Trochet et al., 2004), in a subset of human cases. Conversely, high-powered genome-wide association studies (Capasso et al., 2009; Diskin et al., 2012; Nguyen et al., 2011; Wang et al., 2011) have succeeded in identifying numerous genes that confer a slightly increased risk for the disease. However, the complexity of the disease has confounded the search for druggable pathways. This complexity is illustrated by the current study. We observed a stark variation in tumor susceptibility between two closely related laboratory mouse strains in a relatively tightly controlled model system. Although it is seemingly straightforward, genetic analysis of this variation revealed a strikingly complex system of genetic interactions that required an intensive genomic analysis to decipher. While aggregated genetic evidence implicated the GABA pathway, none of the components were strong enough to be detected alone without an additional genetic interaction, in a well-controlled model system with limited genetic variability compared with human studies. Although the current study was successful in identifying a pharmacologically tractable pathway for therapeutic intervention, it illustrates the difficulty of identifying and characterizing the complex biochemical pathways that influence tumor development.

Arginase inhibitors are under investigation for highly prevalent diseases such as hypertension (Durante et al., 2007). Even more encouragingly, QHii066, the GABA agonist used in this study, is closely related to the benzodiazepine diazepam (Valium), with a similar mechanism of action. The findings that GABA is implicated in neuroblastoma growth and that a benzodiazepine derivative can induce apoptosis raise the possibility that numerous clinically approved drugs used in neurology and psychology can also be used as chemotherapeutic agents. These results also highlight a possible connection between the role of neurotransmitters in nervous system development and the regulation of neuroblastoma growth.

EXPERIMENTAL PROCEDURES

Mice

All mice were obtained from The Jackson Laboratory and were housed and treated in accordance with UCSF IACUC guidelines. Backcross mice were generated by crossing *TH-MYCN* transgenic FVB/N mice to wild-type 129/SvJ and subsequently crossing F1 offspring to wild-type 129/SvJ. Mice were observed for at least 1 year before they were considered tumor free. Tumor-negative backcross mice were followed until 1 year of age (the latest tumor was detected at 342 days). SCGs were surgically isolated and snap-frozen in liquid nitrogen. SCGs were isolated from parental control groups at 21 days.

Taqman Analysis of Transgene Expression

Taqman expression analysis was performed on six mice (three female and three male) from each strain. Proprietary assays for human MYCN and controls L18 and mGUS were obtained from Applied Biosystems. MYCN relative to mGUS is shown in Figure S1B.

Genotyping

DNA was isolated from spleen tissue using a proteinase K lysis followed by phenol chloroform extraction. Microsatellite marker genotyping was carried out by the Marshfield Clinic (Marshfield, WI) and CIDR (Baltimore, MD). SNP genotyping was performed using template-directed primer extension with fluorescence polarization detection (FP-TDI [Hsu et al., 2001], Acycloprime II; Perkin Elmer) and SNPStream (Bell et al., 2002) 48-plex (Beckman Coulter). Markers and map positions are shown in Table S1. The marker set had an average spacing of 8 Mb genome-wide (excluding the high density of markers on chromosome 10).

Linkage Analysis

Interval mapping was performed using the R/qtl (Broman et al., 2003) package in the R statistical language. Genotypes flagged as probable errors by R/qtl were discarded. The genetic map positions were determined using the physical map positions (NCBI 37/mm9) followed by re-estimation of the map using R/qtl, and likely mismapped markers were discarded. Linkage analysis was performed on a 1 cM grid. Genome-wide significance thresholds were determined by running 1,000 permutations for each data set. Interval analysis was performed using the binary mode of the "EM" model. All results reported as significant were significant at a 5% genome-wide error rate, and 95% CIs were determined using the lodint function in R/qtl. Genes within the CIs were determined by counting all genes in the UCSC genome assembly mapping between markers flanking the 95% CI.

Expression Arrays

We isolated RNA from SCGs using the RNeasy kit (QIAGEN) because we found that the buffers in this kit were more effective at disrupting the ganglia than Trizol. We used 1 μg of RNA as a starting template for the RiboMinus rRNA subtraction (Invitrogen), followed by the ST labeling protocol (Affymetrix). Labeled samples were hybridized to Affymetrix Mouse Exon 1.0 arrays. Array quality control was performed using the Affymetrix Expression Console. Two-way comparisons between homogeneous groups (e.g., male versus females or 129/SvJ versus FVB/N males) were performed using the SAM package (Tusher et al., 2001) with a 5% false discovery rate (FDR). Results are presented in Table S3 and plotted in Figures S1C and S1D.

eQTL Analysis

Arrays were normalized using RMA in the XPS package (http://www.bioconductor.org/packages/2.6/bioc/html/xps.html). eQTLs were calculated as described previously (Quigley et al., 2009). Briefly, linkage between gene expression and loci was assessed by linear regression, and genome-wide significance was assessed using a FDR-based method.

Cell Lines and Reagents

Neuroblastoma cell lines were obtained from ATCC. Cells were grown in RPMI media with 10% fetal bovine serum and antibiotics, with the exception of SK-N-BE(2) (Dulbecco's modified Eagle's medium [DMEM]/F12, 10% serum) and IMR-32 (DMEM, 10% serum plus nonessential amino acids). Nor-NOHA

Figure 4. Expression of GABA Genes Correlates with Survival in Human Neuroblastomas

(A–G) Survival curves based on the data set from Asgharzadeh et al. (2006) (available at http://home.ccr.cancer.gov/oncology/oncogenomics) are shown for (A) the GABA-B receptor, (B) *DBI*, (C) *Trak1*, (D) *GABRA-3*, (E) *SLC6A1*, (F) *OAT*, and (G) *ARG1*.

(H) Plot of *ARG1* expression levels for all tumors arranged from highest to lowest along the x axis, showing relatively homogeneous expression levels.

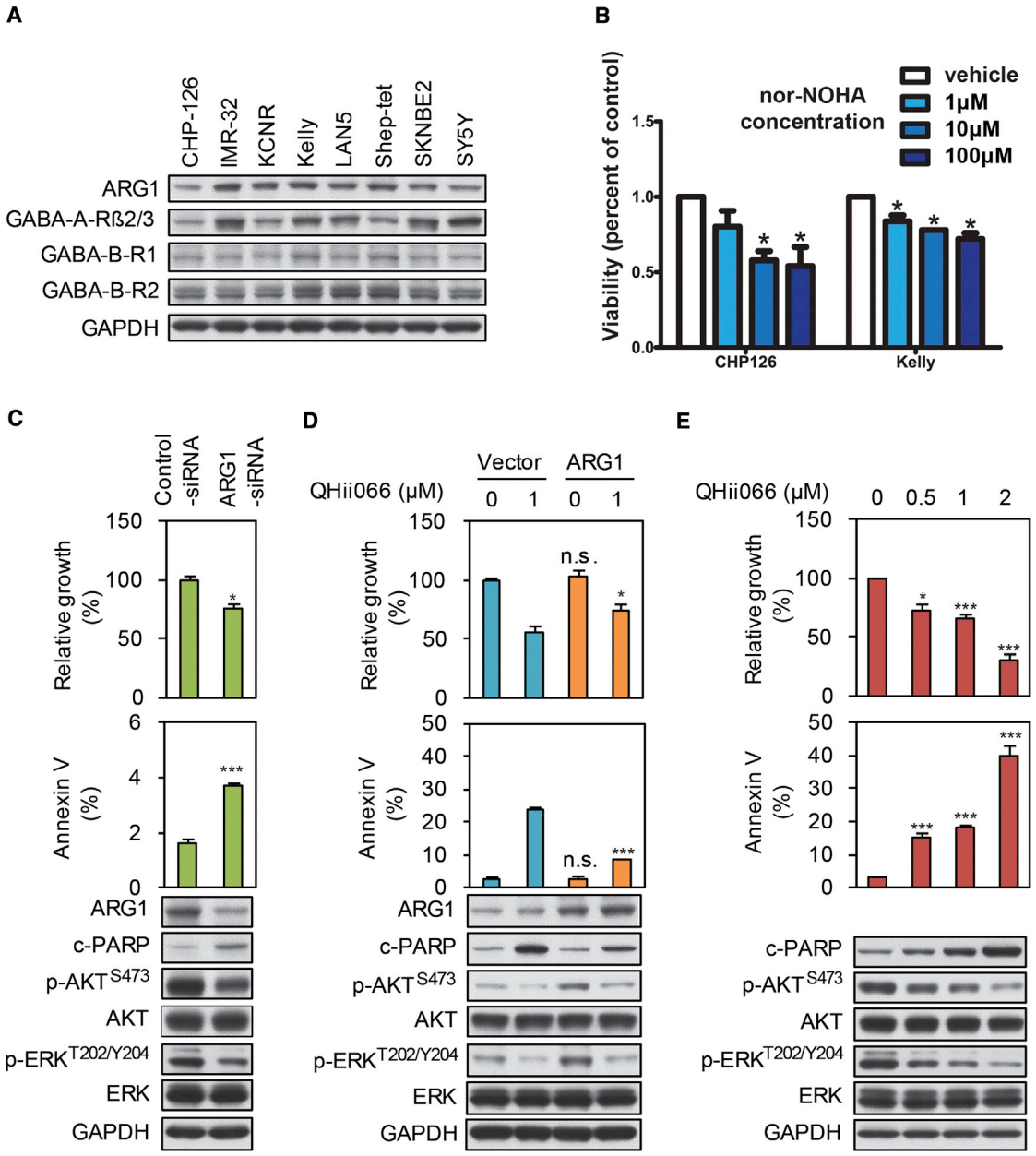

Figure 5. ARG1 Inhibition and GABA Activation Suppress Neuroblastoma Cell Growth and Survival

(A) Expression of ARG1, GABA-A, and GABA-B receptors in neuroblastoma cell lines. Cell lines (as indicated) were harvested, lysed, and analyzed by western blot using the antisera indicated.

(B) WST-1 assay showing a dose-dependent decrease in viability following 72 hr treatment of neuroblastoma cells with varying doses of the ARG1 inhibitor nor-NOHA.

(C) LAN5 cells were transfected with either control or ARG1 siRNA. Cell viability was measured by WST-1. Apoptosis was measured by flow cytometry for the apoptotic marker annexin V. An aliquot of cells was analyzed by immunoblot using the antisera indicated.

(D) LAN-5-pBABE-vector and LAN-5-pBABE-ARG1 cells were treated with DMSO or with the GABA-A agonist QHii066. Cell viability, apoptosis, and protein markers were measured as in (C).

(E) LAN-5 cells were treated with the GABA-A agonist QHii066 for 3 days. Cell viability, apoptosis, and protein markers were measured as in (C).

In (B)–(E), the data shown are mean ± SD of triplicate measurements. NS, not significant versus control/vehicle using Student's t test; *$p < 0.05$, ***$p < 0.001$. See also Figure S4.

was obtained from Bachem and dissolved in DMSO. QHii066 was synthesized at the University of Wisconsin-Milwaukee as described previously (United States Patent US 7,119,196B2).

Western Blotting

Equal amounts of total protein were loaded for 4%–12% SDS-PAGE and transferred to nitrocellulose membranes. After blocking, the membranes

were blotted with ARG1 (R&D Systems), GABA B R1, Erk (Santa Cruz Biotech), GABA A Rβ2/3, GABA B R2, β-tubulin (Millipore), cleaved-PARP (Asp214), p-Akt (Ser473), Akt, pErk (Thr202/Tyr204) (Cell Signaling Technology), and GAPDH (Upstate Biotechnology). Antibodies were detected with horseradish peroxidase-linked anti-mouse, anti-rabbit (Amersham/GE), or anti-sheep immunoglobulin G (Calbiochem/EMD) followed by enhanced chemiluminescence (Amersham/GE).

siRNA Transfection

Control siRNA (Santa Cruz Biotechnology) and Arg1 siRNA (Dharmacon) were transfected using Lipofectamine 2000 (Invitrogen). Cells were harvested for analysis after 72 hr.

Retroviral Transduction

Human *ARG1* cDNA was obtained from the I.M.A.G.E. Consortium, cloned into pENTR4 vector (Invitrogen), and then subcloned into a GATEWAY-compatible pBABE vector. To generate retrovirus, the packaging cell line HEK293T was cotransfected with pBABE vector or pBABE-*ARG1*, along with plasmids expressing gag/pol and vesicular stomatitis virus glycoprotein, using Effectene transfection reagent (QIAGEN). At 48 hr posttransfection, the viral supernatants were filtered and used to infect cells. LAN-5 and Kelly cells were transduced and selected for 2 weeks with 0.5 μg/ml puromycin. Cells were harvested for analysis after 72 hr of subsequent treatment.

Viability

Cells were seeded in 12-well plates and treated as indicated for 48 hr. Viability was determined using the WST-1 assay (Roche) and analyzed by spectrophotometric analysis (absorbance at 450 nm) after 60 min.

Flow Cytometry

Cells were plated on six-well dishes and treated as indicated for 24 hr. They were then harvested, fixed in 70% ethanol for 30 min, and stained with 5 μg/ml propidium iodide containing 125 U/ml RNase. All samples were analyzed on a FACSCaliber flow cytometer (Becton Dickinson) and DNA histograms were modeled offline using ModFit-LT (Verity Software). Apoptosis was detected by flow cytometry for annexin V-FITC (Annexin V-FITC Detection Kit; BioVision) according to the manufacturer's protocol, using FlowJo software (Tree Star).

ACCESSION NUMBERS

The GEO accession number for the microarray data reported in this paper is GSE59675.

SUPPLEMENTAL INFORMATION

Supplemental Information includes four figures and four tables and can be found with this article online at http://dx.doi.org/10.1016/j.celrep.2014.09.046.

AUTHOR CONTRIBUTIONS

C.S.H. performed the majority of the experiments and data analysis. D.A.Q. performed the eQTL and statistical analysis and helped prepare the manuscript. R.A.W., C.C., J.C., W.C.G., and Y.B. performed biochemical assays. D.D.G., W.C.G., and K.N. assisted with mouse work. L.P., J.C., J.M., and P.K. provided technical support for genotyping data generation and analysis. Y.K.S., J.S.W., J.C., S.K., T.V.D., and J.K. provided technical support for expression array data generation and analysis. S.K.R. synthesized QHii066. J.M.C. and Y.-J.C. helped design biochemical experiments. A.B., J.K., Y.-J.C., J.M.C., and T.V.D. helped design experiments and prepare the manuscript. W.A.W. supervised the project. Q.F. supervised and performed the majority of the in vitro analyses. C.S.H. and W.A.W. designed experiments and wrote the paper.

ACKNOWLEDGMENTS

The authors are grateful to the Marshfield Clinic and CIDR for genotyping, and to Fernando Pardo Manuel de Villena, Gary Churchill, Saunak Sen, Denise Lind, and Roger Nicoll for experimental advice and comments on the manuscript. This work was supported by the March of Dimes; the Concern Foundation; the UCSF Academic Senate; NIH R01CA102321, R01NS055750, P30CA82103, U01CA176287, and an ARRA supplement for R01NS055750 (to W.A.W.); and NIH R01MH046851, MH096463, and NS076517 (to J.M.C.).

Received: March 12, 2014
Revised: August 14, 2014
Accepted: September 25, 2014
Published: October 23, 2014

REFERENCES

Andäng, M., Hjerling-Leffler, J., Moliner, A., Lundgren, T.K., Castelo-Branco, G., Nanou, E., Pozas, E., Bryja, V., Halliez, S., Nishimaru, H., et al. (2008). Histone H2AX-dependent GABA(A) receptor regulation of stem cell proliferation. Nature *451*, 460–464.

Asgharzadeh, S., Pique-Regi, R., Sposto, R., Wang, H., Yang, Y., Shimada, H., Matthay, K., Buckley, J., Ortega, A., and Seeger, R.C. (2006). Prognostic significance of gene expression profiles of metastatic neuroblastomas lacking MYCN gene amplification. J. Natl. Cancer Inst. *98*, 1193–1203.

Bak, S.P., Alonso, A., Turk, M.J., and Berwin, B. (2008). Murine ovarian cancer vascular leukocytes require arginase-1 activity for T cell suppression. Mol. Immunol. *46*, 258–268.

Bell, P.A., Chaturvedi, S., Gelfand, C.A., Huang, C.Y., Kochersperger, M., Kopla, R., Modica, F., Pohl, M., Varde, S., Zhao, R., et al. (2002). SNPstream UHT: ultra-high throughput SNP genotyping for pharmacogenomics and drug discovery. Biotechniques, 70–72, 74, 76–77.

Bello-Fernandez, C., Packham, G., and Cleveland, J.L. (1993). The ornithine decarboxylase gene is a transcriptional target of c-Myc. Proc. Natl. Acad. Sci. USA *90*, 7804–7808.

Brem, R.B., Yvert, G., Clinton, R., and Kruglyak, L. (2002). Genetic dissection of transcriptional regulation in budding yeast. Science *296*, 752–755.

Brodeur, G.M., Seeger, R.C., Schwab, M., Varmus, H.E., and Bishop, J.M. (1984). Amplification of N-myc in untreated human neuroblastomas correlates with advanced disease stage. Science *224*, 1121–1124.

Broman, K.W., Wu, H., Sen, S., and Churchill, G.A. (2003). R/qtl: QTL mapping in experimental crosses. Bioinformatics *19*, 889–890.

Capasso, M., Devoto, M., Hou, C., Asgharzadeh, S., Glessner, J.T., Attiyeh, E.F., Mosse, Y.P., Kim, C., Diskin, S.J., Cole, K.A., et al. (2009). Common variations in BARD1 influence susceptibility to high-risk neuroblastoma. Nat. Genet. *41*, 718–723.

Chesler, L., Goldenberg, D.D., Seales, I.T., Satchi-Fainaro, R., Grimmer, M., Collins, R., Struett, C., Nguyen, K.N., Kim, G., Tihan, T., et al. (2007). Malignant progression and blockade of angiogenesis in a murine transgenic model of neuroblastoma. Cancer Res. *67*, 9435–9442.

Ciani, E., Severi, S., Contestabile, A., Bartesaghi, R., and Contestabile, A. (2004). Nitric oxide negatively regulates proliferation and promotes neuronal differentiation through N-Myc downregulation. J. Cell Sci. *117*, 4727–4737.

Crawford, N.P., Alsarraj, J., Lukes, L., Walker, R.C., Officewala, J.S., Yang, H.H., Lee, M.P., Ozato, K., and Hunter, K.W. (2008a). Bromodomain 4 activation predicts breast cancer survival. Proc. Natl. Acad. Sci. USA *105*, 6380–6385.

Crawford, N.P., Walker, R.C., Lukes, L., Officewala, J.S., Williams, R.W., and Hunter, K.W. (2008b). The Diasporin Pathway: a tumor progression-related transcriptional network that predicts breast cancer survival. Clin. Exp. Metastasis *25*, 357–369.

De Deyn, P.P., Marescau, B., and Macdonald, R.L. (1991). Guanidino compounds that are increased in hyperargininemia inhibit GABA and glycine responses on mouse neurons in cell culture. Epilepsy Res. *8*, 134–141.

Deignan, J.L., Marescau, B., Livesay, J.C., Iyer, R.K., De Deyn, P.P., Cederbaum, S.D., and Grody, W.W. (2008). Increased plasma and tissue guanidino compounds in a mouse model of hyperargininemia. Mol. Genet. Metab. *93*, 172–178.

Diskin, S.J., Capasso, M., Schnepp, R.W., Cole, K.A., Attiyeh, E.F., Hou, C., Diamond, M., Carpenter, E.L., Winter, C., Lee, H., et al. (2012). Common variation at 6q16 within HACE1 and LIN28B influences susceptibility to neuroblastoma. Nat. Genet. *44*, 1126–1130.

Durante, W., Johnson, F.K., and Johnson, R.A. (2007). Arginase: a critical regulator of nitric oxide synthesis and vascular function. Clin. Exp. Pharmacol. Physiol. *34*, 906–911.

Ewart-Toland, A., Briassouli, P., de Koning, J.P., Mao, J.H., Yuan, J., Chan, F., MacCarthy-Morrogh, L., Ponder, B.A., Nagase, H., Burn, J., et al. (2003). Identification of Stk6/STK15 as a candidate low-penetrance tumor-susceptibility gene in mouse and human. Nat. Genet. *34*, 403–412.

Gerner, E.W., and Meyskens, F.L., Jr. (2004). Polyamines and cancer: old molecules, new understanding. Nat. Rev. Cancer *4*, 781–792.

Gilbert, S.L., Zhang, L., Forster, M.L., Anderson, J.R., Iwase, T., Soliven, B., Donahue, L.R., Sweet, H.O., Bronson, R.T., Davisson, M.T., et al. (2006). Trak1 mutation disrupts GABA(A) receptor homeostasis in hypertonic mice. Nat. Genet. *38*, 245–250.

Gray, P.W., Glaister, D., Seeburg, P.H., Guidotti, A., and Costa, E. (1986). Cloning and expression of cDNA for human diazepam binding inhibitor, a natural ligand of an allosteric regulatory site of the gamma-aminobutyric acid type A receptor. Proc. Natl. Acad. Sci. USA *83*, 7547–7551.

Hackett, C.S., Hodgson, J.G., Law, M.E., Fridlyand, J., Osoegawa, K., de Jong, P.J., Nowak, N.J., Pinkel, D., Albertson, D.G., Jain, A., et al. (2003). Genome-wide array CGH analysis of murine neuroblastoma reveals distinct genomic aberrations which parallel those in human tumors. Cancer Res. *63*, 5266–5273.

Hale, G., Gula, M.J., and Blatt, J. (1994). Impact of gender on the natural history of neuroblastoma. Pediatr. Hematol. Oncol. *11*, 91–97.

He, X., Huang, Q., Ma, C., Yu, S., McKernan, R., and Cook, J.M. (2000). Pharmacophore/receptor models for GABA(A)/BzR alpha2beta3gamma2, alpha3beta3gamma2 and alpha4beta3gamma2 recombinant subtypes. Included volume analysis and comparison to alpha1beta3gamma2, alpha5beta3gamma2, and alpha6beta3gamma2 subtypes. Drug Des. Discov. *17*, 131–171.

Hogarty, M.D., Norris, M.D., Davis, K., Liu, X., Evageliou, N.F., Hayes, C.S., Pawel, B., Guo, R., Zhao, H., Sekyere, E., et al. (2008). ODC1 is a critical determinant of MYCN oncogenesis and a therapeutic target in neuroblastoma. Cancer Res. *68*, 9735–9745.

Hsu, T.M., Chen, X., Duan, S., Miller, R.D., and Kwok, P.Y. (2001). Universal SNP genotyping assay with fluorescence polarization detection. Biotechniques *31*, 560, 562, 564–568, passim.

Huang, Q., He, X., Ma, C., Liu, R., Yu, S., Dayer, C.A., Wenger, G.R., McKernan, R., and Cook, J.M. (2000). Pharmacophore/receptor models for GABA(A)/BzR subtypes (alpha1beta3gamma2, alpha5beta3gamma2, and alpha6beta3gamma2) via a comprehensive ligand-mapping approach. J. Med. Chem. *43*, 71–95.

Huang, Y., Higginson, D.S., Hester, L., Park, M.H., and Snyder, S.H. (2007). Neuronal growth and survival mediated by eIF5A, a polyamine-modified translation initiation factor. Proc. Natl. Acad. Sci. USA *104*, 4194–4199.

Janoueix-Lerosey, I., Lequin, D., Brugières, L., Ribeiro, A., de Pontual, L., Combaret, V., Raynal, V., Puisieux, A., Schleiermacher, G., Pierron, G., et al. (2008). Somatic and germline activating mutations of the ALK kinase receptor in neuroblastoma. Nature *455*, 967–970.

Jenkins, D.C., Charles, I.G., Thomsen, L.L., Moss, D.W., Holmes, L.S., Baylis, S.A., Rhodes, P., Westmore, K., Emson, P.C., and Moncada, S. (1995). Roles of nitric oxide in tumor growth. Proc. Natl. Acad. Sci. USA *92*, 4392–4396.

Koomoa, D.L., Yco, L.P., Borsics, T., Wallick, C.J., and Bachmann, A.S. (2008). Ornithine decarboxylase inhibition by alpha-difluoromethylornithine activates opposing signaling pathways via phosphorylation of both Akt/protein kinase B and p27Kip1 in neuroblastoma. Cancer Res. *68*, 9825–9831.

La Merrill, M., Gordon, R.R., Hunter, K.W., Threadgill, D.W., and Pomp, D. (2010). Dietary fat alters pulmonary metastasis of mammary cancers through cancer autonomous and non-autonomous changes in gene expression. Clin. Exp. Metastasis *27*, 107–116.

Le-Corronc, H., Rigo, J.M., Branchereau, P., and Legendre, P. (2011). GABA(A) receptor and glycine receptor activation by paracrine/autocrine release of endogenous agonists: more than a simple communication pathway. Mol. Neurobiol. *44*, 28–52.

MacPhee, M., Chepenik, K.P., Liddell, R.A., Nelson, K.K., Siracusa, L.D., and Buchberg, A.M. (1995). The secretory phospholipase A2 gene is a candidate for the Mom1 locus, a major modifier of ApcMin-induced intestinal neoplasia. Cell *81*, 957–966.

Mao, J.H., Saunier, E.F., de Koning, J.P., McKinnon, M.M., Higgins, M.N., Nicklas, K., Yang, H.T., Balmain, A., and Akhurst, R.J. (2006). Genetic variants of Tgfb1 act as context-dependent modifiers of mouse skin tumor susceptibility. Proc. Natl. Acad. Sci. USA *103*, 8125–8130.

Mosse, Y.P., Laudenslager, M., Khazi, D., Carlisle, A.J., Winter, C.L., Rappaport, E., and Maris, J.M. (2004). Germline PHOX2B mutation in hereditary neuroblastoma. Am. J. Hum. Genet. *75*, 727–730.

Mossé, Y.P., Laudenslager, M., Longo, L., Cole, K.A., Wood, A., Attiyeh, E.F., Laquaglia, M.J., Sennett, R., Lynch, J.E., Perri, P., et al. (2008). Identification of ALK as a major familial neuroblastoma predisposition gene. Nature *455*, 930–935.

Nguyen, le B., Diskin, S.J., Capasso, M., Wang, K., Diamond, M.A., Glessner, J., Kim, C., Attiyeh, E.F., Mosse, Y.P., Cole, K., et al. (2011). Phenotype restricted genome-wide association study using a gene-centric approach identifies three low-risk neuroblastoma susceptibility loci. PLoS Genet. *7*, e1002026.

Park, Y.G., Zhao, X., Lesueur, F., Lowy, D.R., Lancaster, M., Pharoah, P., Qian, X., and Hunter, K.W. (2005). Sipa1 is a candidate for underlying the metastasis efficiency modifier locus Mtes1. Nat. Genet. *37*, 1055–1062.

Quigley, D.A., To, M.D., Pérez-Losada, J., Pelorosso, F.G., Mao, J.H., Nagase, H., Ginzinger, D.G., and Balmain, A. (2009). Genetic architecture of mouse skin inflammation and tumour susceptibility. Nature *458*, 505–508.

Roberts, S.S., Mori, M., Pattee, P., Lapidus, J., Mathews, R., O'Malley, J.P., Hsieh, Y.C., Turner, M.A., Wang, Z., Tian, Q., et al. (2004). GABAergic system gene expression predicts clinical outcome in patients with neuroblastoma. J. Clin. Oncol. *22*, 4127–4134.

Schadt, E.E., Monks, S.A., Drake, T.A., Lusis, A.J., Che, N., Colinayo, V., Ruff, T.G., Milligan, S.B., Lamb, J.R., Cavet, G., et al. (2003). Genetics of gene expression surveyed in maize, mouse and man. Nature *422*, 297–302.

Schwab, M., Varmus, H.E., Bishop, J.M., Grzeschik, K.H., Naylor, S.L., Sakaguchi, A.Y., Brodeur, G., and Trent, J. (1984). Chromosome localization in normal human cells and neuroblastomas of a gene related to c-myc. Nature *308*, 288–291.

Singh, R., Pervin, S., Karimi, A., Cederbaum, S., and Chaudhuri, G. (2000). Arginase activity in human breast cancer cell lines: N(omega)-hydroxy-L-arginine selectively inhibits cell proliferation and induces apoptosis in MDA-MB-468 cells. Cancer Res. *60*, 3305–3312.

Tenu, J.P., Lepoivre, M., Moali, C., Brollo, M., Mansuy, D., and Boucher, J.L. (1999). Effects of the new arginase inhibitor N(omega)-hydroxy-nor-L-arginine on NO synthase activity in murine macrophages. Nitric Oxide *3*, 427–438.

Trochet, D., Bourdeaut, F., Janoueix-Lerosey, I., Deville, A., de Pontual, L., Schleiermacher, G., Coze, C., Philip, N., Frébourg, T., Munnich, A., et al. (2004). Germline mutations of the paired-like homeobox 2B (PHOX2B) gene in neuroblastoma. Am. J. Hum. Genet. *74*, 761–764.

Tusher, V.G., Tibshirani, R., and Chu, G. (2001). Significance analysis of microarrays applied to the ionizing radiation response. Proc. Natl. Acad. Sci. USA *98*, 5116–5121.

Wakabayashi, Y., Mao, J.H., Brown, K., Girardi, M., and Balmain, A. (2007). Promotion of Hras-induced squamous carcinomas by a polymorphic variant of the Patched gene in FVB mice. Nature *445*, 761–765.

Wang, K., Diskin, S.J., Zhang, H., Attiyeh, E.F., Winter, C., Hou, C., Schnepp, R.W., Diamond, M., Bosse, K., Mayes, P.A., et al. (2011). Integrative genomics identifies LMO1 as a neuroblastoma oncogene. Nature *469*, 216–220.

Weiss, W.A., Aldape, K., Mohapatra, G., Feuerstein, B.G., and Bishop, J.M. (1997). Targeted expression of MYCN causes neuroblastoma in transgenic mice. EMBO J. *16*, 2985–2995.

Yachimovich-Cohen, N., Even-Ram, S., Shufaro, Y., Rachmilewitz, J., and Reubinoff, B. (2010). Human embryonic stem cells suppress T cell responses via arginase I-dependent mechanism. J. Immunol. *184*, 1300–1308.

Yang, X., Deignan, J.L., Qi, H., Zhu, J., Qian, S., Zhong, J., Torosyan, G., Majid, S., Falkard, B., Kleinhanz, R.R., et al. (2009). Validation of candidate causal genes for obesity that affect shared metabolic pathways and networks. Nat. Genet. *41*, 415–423.

Yu, H., Iyer, R.K., Kern, R.M., Rodriguez, W.I., Grody, W.W., and Cederbaum, S.D. (2001). Expression of arginase isozymes in mouse brain. J. Neurosci. Res. *66*, 406–422.

Yu, H., Iyer, R.K., Yoo, P.K., Kern, R.M., Grody, W.W., and Cederbaum, S.D. (2002). Arginase expression in mouse embryonic development. Mech. Dev. *115*, 151–155.

Yu, H., Yoo, P.K., Aguirre, C.C., Tsoa, R.W., Kern, R.M., Grody, W.W., Cederbaum, S.D., and Iyer, R.K. (2003). Widespread expression of arginase I in mouse tissues. Biochemical and physiological implications. J. Histochem. Cytochem. *51*, 1151–1160.